Multi-spacecraft Intelligent Orbit Phasing Control Considering Collision Avoidance

*LI Jian, ZHANG Gang**

Research Center of Satellite Technology, Harbin Institute of Technology, Harbin 150080, P. R. China

(Received 16 June 2022; revised 8 August 2022; accepted 13 August 2022)

Abstract: This paper proposes an intelligent low-thrust orbit phasing control method for multiple spacecraft by simultaneously considering fuel optimization and collision avoidance. Firstly, the minimum-fuel orbit phasing control database is generated by the indirect method associated with the homotopy technique. Then, a deep network representing the minimum-fuel solution is trained. To avoid collision for multiple spacecraft, an artificial potential function is introduced in the collision-avoidance controller. Finally, an intelligent orbit phasing control method by combining the minimum-fuel neural network controller and the collision-avoidance controller is proposed. Numerical results show that the proposed intelligent orbit phasing control is valid for the multi-satellite constellation initialization without collision.

Key words: orbit phasing control; low thrust; deep neural networks; collision avoidance

CLC number: V448.2 **Document code**: A **Article ID**: 1005-1120(2022)04-0379-10

0 Introduction

In recent years, the number of on orbit spacecraft increases rapidly, thus it is important to develop the intelligent autonomous control scheme of spacecraft. Due to high specific impulse and high precision, low-thrust thrusters such as electric propulsion are important ways for orbit control. Therefore, the low-thrust trajectory optimization problem has attracted many attentions. The low-thrust trajectory optimization methods mainly include the direct method[1], the indirect method[2], and the shape-based method[3]. Compared with the other two methods, the indirect method can guarantee the first-order optimality condition, but it is sensitive to initial values. Generally speaking, the shape-based method and the direct method can be used to provide the initial guess[4], and the homotopy technique[5-6] can be used to reduce the difficulty for the initial guess. However, traditional methods need complex numerical calculations, and they cannot be used on board.

Recently, the intelligent technology represented by the deep neural network and the machine learning provides a new way to solve the low-thrust trajectory optimization problem. The powerful fitting ability of the deep neural network is used to provide an initial guess for the costate variable in the indirect method[7-8], but the exact value of the initial costate variable also needs to be solved by numerical iterations. In addition, the neural network can be directly used to obtain the optimal control[9-11]. For the training data in neural networks, Cheng et al.[10] used an actor-indirect method to employ a network learning architecture, and Izzo et al.[11] proposed a new general methodology called "backward generation of optimal examples" to create the database. Compared with the traditional methods, the preced-

*Corresponding author, E-mail address: zhanggang@hit.edu.cn.

How to cite this article: LI Jian, ZHANG Gang. Multi-spacecraft intelligent orbit phasing control considering collision avoidance[J]. Transactions of Nanjing University of Aeronautics and Astronautics, 2022, 39(4): 379-388.

http://dx.doi.org/10.16356/j.1005-1120.2022.04.001

ing intelligent studies do not need complex numerical calculations, but they are not valid for multiple spacecraft.

For the multi-spacecraft control, two important objectives are fuel optimization and collision avoidance. For the fuel optimal control problems, the model predictive control method and the convex optimization method are used for multiple spacecraft[12]. However, the computational burden of this method increases significantly for large number of spacecraft and long transfer time. Therefore, it is not suitable for on-board applications. For the collision avoidance problem, each spacecraft need to have the autonomous control capability, thus the artificial potential function (APF) is widely used in the control design[13-14]. In addition, another idea is to combine the sliding mode control with the APF control to realize the closed-loop multi-satellite control under the collision constraint[15-17]. However, all preceding methods are based on the relative dynamic model. For the absolute dynamic model, Yu et al.[18] proposed a quadratic APF controller to achieve the spacecraft autonomous cluster without collision, but they did not consider the fuel optimality in the control process. In summary, there is no control method considering both the fuel optimality and the collision constraint.

The main contribution of this paper is to provide an intelligent autonomous orbit phasing control method by simultaneously considering the fuel optimization and the collision avoidance. This paper is structured as follows: In Section 1, the dynamic model is introduced and the indirect optimal control method is given; in Section 2, the database generation method with the homotopy technique, and the design and training process of neural network are proposed; then, the minimum-fuel neural network controller is combined with the collision-avoidance controller in Section 3; in Section 4, two numerical examples are provided; finally, the conclusions are given in Section 5.

1 Low-Thrust Trajectory Optimization

1.1 Dynamic model

The cylindrical coordinate system is shown in Fig.1, where r, θ and z are the radial distance, the azimuth angle, and the altitude of the spacecraft, respectively.

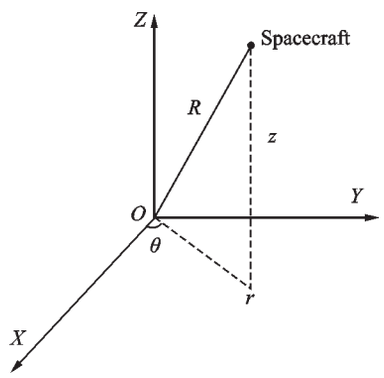

Fig.1 Cylindrical coordinates

The motion of spacecraft can be described as the following differential equation[19]

$$\begin{cases} \dot{\boldsymbol{x}} = \boldsymbol{D} + \dfrac{T_{\max} u}{m} \boldsymbol{B}\boldsymbol{\alpha} \\ \dot{m} = -\dfrac{T_{\max} u}{I_{\mathrm{sp}} g_0} \end{cases} \tag{1}$$

where

$$\boldsymbol{D} = \begin{bmatrix} v_r \\ v_\theta \\ v_z \\ v_\theta^2 r - \mu r / R^3 \\ -2 v_r v_\theta / r \\ -\mu z / R^3 \end{bmatrix}, \quad \boldsymbol{B}^{\mathrm{T}} = \begin{bmatrix} 0 & 0 & 0 & 1 & 0 & 0 \\ 0 & 0 & 0 & 0 & 1/r & 0 \\ 0 & 0 & 0 & 0 & 0 & 1 \end{bmatrix} \tag{2}$$

and $\boldsymbol{x} = [r, \theta, z, v_r, v_\theta, v_z]^{\mathrm{T}}$, here v_r, v_θ and v_z are the derivatives of r, θ and z, respectively; $\boldsymbol{\alpha} = [\alpha_r, \alpha_\theta, \alpha_z]$ is the thrust direction; m is the mass; I_{sp} is the specific impulse of thruster; $\mu = 398\,600.441\,5\ \mathrm{km}^3/\mathrm{s}^2$ is the gravitational constant; $g_0 = 9.806\,65\ \mathrm{m/s}^2$ is the gravitational acceleration at sea level; $u = T/T_{\max}$, and $u \in [0, 1]$ is the engine thrust ratio, here T and $T_{\max}$ are the current and maximum thrust magnitudes, respectively; $R = \sqrt{r^2 + z^2}$ is the distance from the center of the space-

craft to the Earth.

This paper mainly stuides the orbit phasing control in the phase initialization and phase reconfiguration missions for the multi-satellite constellation. For different satellites in the same orbit (with the same semi-major axis, eccentricity and inclination), the right ascension of the ascending node (RAAN) change rates caused by J2 perturbation are almost the same. Thus, the J2 perturbation is ignored in the orbit phasing control here.

1.2 Optimal control problem

For the fuel optimal orbit phasing control problem with free transfer time t_f, the performance index can be expressed as

$$J=\frac{T_{\max}}{I_{sp}g_0}\int_0^{t_f}u\,\mathrm{d}t \tag{3}$$

To overcome the difficulty arising from solving the bang-bang control, the homotopic approach is adopted in the performance index, so we have

$$J=\frac{T_{\max}}{I_{sp}g_0}\int_0^{t_f}[u-\varepsilon u(1-u)]\,\mathrm{d}t \tag{4}$$

where $\varepsilon\in[0,1]$ is the homotopy parameter. As the ε decreases from 1 to 0, the problem changes from the easily solved energy optimal problem into the fuel optimal control problem. When $\varepsilon=0$, the problem is the fuel optimal problem.

$$\boldsymbol{M}(\boldsymbol{x})=\begin{bmatrix}0&0&0&1&0&0\\0&0&0&0&1&0\\0&0&0&0&0&1\\\dot\theta^2+\dfrac{\mu(3r^2-R^2)}{R^5}&0&3\dfrac{\mu rz}{R^5}&0&2r\dot\theta&0\\\dfrac{2\dot r\dot\theta-a_\theta}{r^2}&0&0&-\dfrac{2\dot\theta}{r}&-\dfrac{2\dot r}{r}&0\\3\dfrac{\mu rz}{R^5}&0&\mu\dfrac{(3r^2-R^2)}{R^5}&0&0&0\end{bmatrix} \tag{10}$$

Since the transfer time of the spacecraft is free, there are two additional boundary conditions, i.e.

$$H(t_f)=0,\quad \lambda_m(t_f)=0 \tag{11}$$

Then, the two-point boundary value problem in the cylindrical coordinate system with the homotopy parameter is obtained, and the corresponding shooting equation is

$$\Phi(\boldsymbol{\Lambda}_\varepsilon)=\left[|\boldsymbol{x}_c(t_f)-\boldsymbol{x}_t(t_f)|;\lambda_m(t_f);H(t_f)\right]^{\mathrm{T}}=0 \tag{12}$$

For the performance index in Eq.(4), the following Hamiltonian function is constructed by introducing the costate variable $\boldsymbol{\lambda}$.

$$H=\frac{T_{\max}}{I_{sp}g_0}[u-\varepsilon u(1-u)]+\boldsymbol{\lambda}_x^{\mathrm{T}}\boldsymbol{D}+\boldsymbol{\lambda}_x^{\mathrm{T}}\left(\frac{T_{\max}u}{m}\boldsymbol{B}\boldsymbol{\alpha}\right)-\lambda_m\frac{T_{\max}u}{I_{sp}g_0} \tag{5}$$

where $\boldsymbol{\lambda}_x^{\mathrm{T}}=[\lambda_r,\lambda_\theta,\lambda_z,\lambda_{v_r},\lambda_{v_\theta},\lambda_{v_z}]$. In order to minimize the Hamiltonian function H, the optimal thrust direction $\boldsymbol{\alpha}^*$ is

$$\boldsymbol{\alpha}^*=-\frac{[\boldsymbol{\lambda}_x^{\mathrm{T}}\boldsymbol{B}]^{\mathrm{T}}}{\|\boldsymbol{\lambda}_x^{\mathrm{T}}\boldsymbol{B}\|} \tag{6}$$

and the optimal thrust magnitude ratio u^* is

$$u^*=\begin{cases}0 & \rho>\varepsilon\\1 & \rho<-\varepsilon\\0.5-\rho/2\varepsilon & |\rho|\leqslant\varepsilon\end{cases} \tag{7}$$

where ρ is the switching function, shown as

$$\rho=1-\frac{\|\boldsymbol{\lambda}_x^{\mathrm{T}}\boldsymbol{B}\|I_{sp}g_0}{m}-\lambda_m \tag{8}$$

The differential equation of the costate variable $\boldsymbol{\lambda}$ is

$$\begin{cases}\dot{\boldsymbol{\lambda}}_x=-\dfrac{\partial H}{\partial x}=\boldsymbol{M}(\boldsymbol{x})\boldsymbol{\lambda}_x\\\dot\lambda_m=-\dfrac{T_{\max}u}{m^2}\|\boldsymbol{\lambda}_x^{\mathrm{T}}\boldsymbol{B}\|u\end{cases} \tag{9}$$

where $\boldsymbol{\Lambda}_\varepsilon=[\lambda_{r_i},\lambda_{\theta_i},\lambda_{z_i},\lambda_{v_{r_i}},\lambda_{v_{\theta_i}},\lambda_{v_{z_i}},\lambda_{m_i},t_f]$ is the variable needs to be solved, and $\boldsymbol{x}_c$ and $\boldsymbol{x}_t$ are the states of the chaser and the target, respectively.

2 Network Training

This section describes the methods for the data generation, the neural network architecture and the training method. The purpose is to obtain a mini-

mum-fuel neural network controller for the autonomous fuel-optimal control in real time.

2.1 Training data generation

In order to realize the minimum-fuel neural network controller, the input of the network includes the current state $\boldsymbol{x}_{ci}$, the current mass m_{ci} and the expected state $\boldsymbol{x}_{ti}$. The output is the optimal control variable $\boldsymbol{U}^*=(u,\theta_r,\theta_z)$, where $\theta_r\in[-\pi,\pi]$, $\theta_z\in[-\pi/2,\pi/2]$ are the thrust direction angles. The thrust direction angles can be expressed as

$$\begin{cases}\theta_r=\arctan\left(\dfrac{\alpha_\theta}{\alpha_r}\right)\\ \theta_z=\arcsin(\alpha_z)\end{cases}\tag{13}$$

In this way, we can combine the spacecraft state and the control to construct a set of training data $(\boldsymbol{x}_{ci},m_{ci},\boldsymbol{x}_{ti},\boldsymbol{U}^*)$.

Based on the optimal solution by the homotopy technique, a database can be generated. By perturbing the initial state of the nominal trajectory, the undisturbed state can provide a good initial guess for the disturbed state. For the nominal optimal trajectory, the initial and terminal states are $\boldsymbol{x}_{cio}^*$ and $\boldsymbol{x}_{tio}^*$, respectively, and the optimal costate variable is $\boldsymbol{\Lambda}^*$. A new set of values of the initial state $\boldsymbol{x}_{cio}^{new}$ and the expected state $\boldsymbol{x}_{tio}^{new}$ is

$$\boldsymbol{x}_{cio}^{new}=\boldsymbol{x}_{cio}^*+\delta\boldsymbol{x}_{co},\ \boldsymbol{x}_{tio}^{new}=\boldsymbol{x}_{tio}^*+\delta\boldsymbol{x}_{to}\tag{14}$$

where $\boldsymbol{x}_{cio}^{new}$, $\boldsymbol{x}_{cio}^*$, $\boldsymbol{x}_{tio}^{new}$ and $\boldsymbol{x}_{tio}^*$ are all states given in the form of orbital elements. The orbital elements include the semimajor axis of the nominal orbit a, the eccentricity e, the inclination i, the RAAN Ω, the argument of perigee ω and the true anomaly φ. In addition, $\delta\boldsymbol{x}_{co}$ and $\delta\boldsymbol{x}_{to}$ represent small enough disturbances, so that the shooting equation solution $\boldsymbol{\Lambda}^*$ in the original states can be used as the initial guess to solve the solution $\boldsymbol{\Lambda}^{new*}$ of the shooting equation in the new states. Since $\delta\boldsymbol{x}_{co}$ and $\delta\boldsymbol{x}_{to}$ are small, the initial guess is close to the optimal value, and the shooting method can converge quickly.

In the above process, firstly the true anomaly φ in the range $[0,360^\circ)$ is divided into 500 equal values, and the homotopy method is used to solve the optimal orbits at different phases, which are viewed as the nominal orbits with different phases. Then, for these nominal orbits, the other five orbit elements are disturbed to obtain many optimal solutions. Finally, all the obtained optimal orbits are combined to establish the optimal control database.

2.2 Network structure selection

In this paper, two kinds of neural networks are established. The first one is the thrust-ratio network, which predicts the thrust ratio u. Note that u of the fuel optimal control is only 0 or 1, and we establish a classified neural network to fit the thrust magnitude term in the control. The second one is the thrust-direction-angle network, which is to predict the thrust direction angles θ_r and θ_z.

Due to the strong nonlinearity of the optimal control, the network needs to have a certain complexity to capture the relationship between the optimal control and the state. Therefore, to avoid under fitting and over fitting for the thrust ratio, a neural network is designed with three hidden layers and 128 neurons in each layer for the control magnitude network. To realize the fitting of the thrust direction angles, a neural network is designed with nine hidden layers and 128 neurons in each layer. The specific structure of the network is Fig.2.

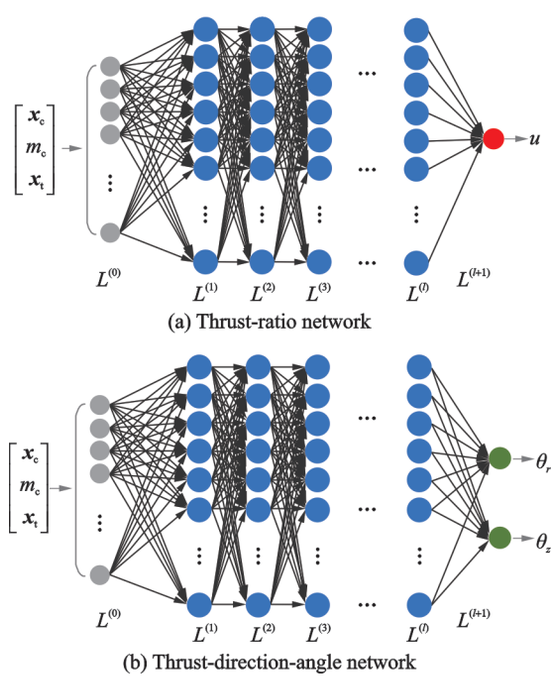

Fig.2 Minimum-fuel neural network architecture

2.3 Selection of activation function and loss function

This subsection mainly introduces the architecture design of neural network and the selection of activation-function.

Firstly, the fully connected feedforward network is selected. The activation function of the output layer is determined according to the range of the output. For the thrust-ratio network, the Sigmoid function is used as the activation function of the output layer. For the thrust-direction-angle network, the Tanh function is selected as the activation function of the output layer. For the hidden layer of the network, the ReLU function is selected as the activation function.

Then, the mean square error (MSE) between the training data and the network prediction results is adopted as the loss function, shown as

$$L(\boldsymbol{\omega},\boldsymbol{b})=\frac{1}{N}\sum_{i=1}^{N}\left\|\operatorname{Net}(\boldsymbol{X}_i|\boldsymbol{\omega},\boldsymbol{b})-\hat{\boldsymbol{Y}}_i\right\|^2 \quad (15)$$

where the Net function is the neural network to be trained, and N represents the total number of samples used for training. The input vector $\boldsymbol{X}_i$ is composed of the states, the target vector $\hat{\boldsymbol{Y}}_i$ contains the optimal control to be learned, and the symbols $\boldsymbol{\omega}$ and $\boldsymbol{b}$ denote the weight and bias of network, respectively. In addition, to avoid system memory explosion caused by all data input into the network, the batch size is set to be 500.

3 Collision Avoidance

When multiple spacecraft are controlled simultaneously, the collision risk increases. To avoid collision, this section proposes a collision-avoidance method based on the APF.

3.1 Control process

In order to avoid collision, the repulsive field is introduced to prevent spacecraft collision during maneuvers. Assume that the collision between spacecraft is given in the form of distance. In this way, when there is no collision risk between spacecraft, it uses the optimal control obtained by neural network; however, when there is collision risk, the APF is used to avoid collision. The control process of spacecraft is shown in Fig.3, and the steps are given as follows.

Step 1 Judge whether the current state of the spacecraft meets the terminal constraints. If no, use the intelligent controller generated in Section 2.

Step 2 If the spacecraft meets the terminal constraints or is being controlled by the artificial intelligence controller, judge whether there is a collision risk. If yes, it needs to use the APF to avoid collision.

Step 3 If the spacecraft has no collision risk or execute the collision-avoidance maneuver, it is necessary to judge whether it meets the terminal constraint again. If yes, the control is completed. If no, return to Step 1 and repeat the above process. Until all spacecraft meet the terminal constraints and there is no collision risk, the control is over.

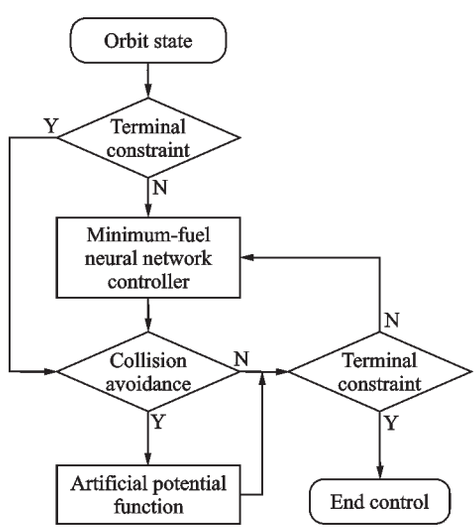

Fig.3 Flow chart of the controller

3.2 Artificial potential function design

In the terminal constraints in Fig.3, the safety constraints of spacecraft are expressed as

$$\|\boldsymbol{r}_{\min}\|>L \quad (16)$$

where $\boldsymbol{r}_{\min}$ represents the nearest distance among all spacecraft and L the allowable minimum distance between spacecraft. The APF of the spacecraft from

the nearest spacecraft is

$$U_o(\boldsymbol{x}_i,\boldsymbol{x}_j)=\begin{cases}0.5k\left(\dfrac{1}{\|\boldsymbol{r}_{\min}\|}-\dfrac{1}{d_0}\right) & \|\boldsymbol{r}_{\min}\|\leqslant d_0\\ 0 & \|\boldsymbol{r}_{\min}\|>d_0\end{cases} \tag{17}$$

where d_0 is the radius of the APF. When the distance between spacecraft is less than d_0, there is a risk of collision between them. Then, the repulsion force magnitude to the spacecraft is

$$F_o(\boldsymbol{x}_i,\boldsymbol{x}_j)=-\nabla U_o(\boldsymbol{x}_i,\boldsymbol{x}_j)=\begin{cases}\dfrac{k}{\|\boldsymbol{r}_{\min}\|^2}\left(\dfrac{1}{\|\boldsymbol{r}_{\min}\|}-\dfrac{1}{d_0}\right) & \|\boldsymbol{r}_{\min}\|\leqslant d_0\\ 0 & \|\boldsymbol{r}_{\min}\|>d_0\end{cases} \tag{18}$$

where k is the gain coefficient. The influence of APF on energy consumption in the whole control process can be changed by adjusting the gain coefficient k. Because the spacecraft will fly by other spacecraft during the whole period, the safe distance between spacecraft can be ensured by changing the semi-major axis.

Note that the semi-major axis does not change under the acceleration component perpendicular to the tangential direction in the orbit plane. Then, this paper mainly uses the tangential acceleration component to change the semi-major axis to achieve the purpose of collision avoidance. Assume that the tangential acceleration direction of spacecraft S_i is α_{ui}. Thus, α_{ui} can be expressed as

$$\alpha_{ui}=\begin{cases}-1 & (a_j-a_i)>da_0\\ 1 & (a_i-a_j)>da_0\\ 0 & -da_0\leqslant(a_i-a_j)\leqslant da_0\end{cases} \tag{19}$$

where a_i is the semi-major axis of the spacecraft S_i, and da_0 represents the deviation limit of the semi-major axis to prevent the thrust direction oscillation caused by the small difference of semi-major axis. The tangential acceleration vector can be written in the coordinate system $[S,\ T,\ W]$, which denotes the radial, transverse and normal directions, respectively. Then, we have

$$\begin{cases}S=A\alpha_{ui}\\ T=B\alpha_{ui}\\ W=0\end{cases} \tag{20}$$

where

$$A=\frac{e\sin\varphi}{\sqrt{1+2e\cos\varphi+e^2}},\ B=\frac{1+e\cos\varphi}{\sqrt{1+2e\cos\varphi+e^2}} \tag{21}$$

Then, the next step is to transform the frame $[S,T,W]^{\mathrm{T}}$ into the geocentric inertial coordinate system, shown as

$$\begin{bmatrix}a_x\\ a_y\\ a_z\end{bmatrix}=\boldsymbol{R}_3(-\Omega)\boldsymbol{R}_1(-i)\boldsymbol{R}_3(-\omega-\varphi)\begin{bmatrix}S\\ T\\ W\end{bmatrix} \tag{22}$$

where $\boldsymbol{R}_1(\vartheta)$ and $\boldsymbol{R}_3(\vartheta)$ represent rotation matrices that rotate vectors by the angle ϑ about the X- and Z-axes, respectively[20]. The acceleration direction in the cylindrical coordinate system $\boldsymbol{\alpha}_{O\text{-}r\theta z}=[\alpha_r,\alpha_\theta,\alpha_z]^{\mathrm{T}}$ can be obtained as

$$\begin{cases}\alpha_r=\alpha_x\cos\theta+\alpha_y\sin\theta\\ \alpha_\theta=-\alpha_x\sin\theta+\alpha_y\cos\theta\\ \alpha_z=\alpha_z\end{cases} \tag{23}$$

The outputs of the neural network are $[u_{\mathrm{net}},\theta_r,\theta_z]$. Thus, the acceleration direction vector of the spacecraft is $\boldsymbol{\alpha}_{\mathrm{net}}=[\alpha_{\mathrm{net}_r},\alpha_{\mathrm{net}_\theta},\alpha_{\mathrm{net}_z}]^{\mathrm{T}}$, and

$$\begin{cases}\alpha_{\mathrm{net}_r}=\cos\theta_z\cos\theta_r\\ \alpha_{\mathrm{net}_\theta}=\cos\theta_z\sin\theta_r\\ \alpha_{\mathrm{net}_z}=\sin\theta_z\end{cases} \tag{24}$$

By combining this acceleration and that by the minimum-fuel neural network controller, the final normalized acceleration $\hat{\boldsymbol{u}}$ to avoid collision is

$$\hat{\boldsymbol{u}}=u\boldsymbol{\alpha}=\frac{F_o(\boldsymbol{x}_i,\boldsymbol{x}_j)\cdot\boldsymbol{\alpha}_{O\text{-}r\theta z}+u_{\mathrm{net}}\boldsymbol{\alpha}_{\mathrm{net}}}{\|F_o(\boldsymbol{x}_i,\boldsymbol{x}_j)\cdot\boldsymbol{\alpha}_{O\text{-}r\theta z}+u_{\mathrm{net}}\boldsymbol{\alpha}_{\mathrm{net}}\|} \tag{25}$$

3.3 State deviation and control limit

To describe whether the spacecraft reaches the expected state, the subsection will give the calculation method of control limit, in which the state deviations of the spacecraft are given in the form of cylindrical coordinates, and its expression is

$$\begin{cases}|\Delta r|=|r_{\mathrm{f}}-r|,\quad |\Delta v_r|=|v_{r_{\mathrm{f}}}-v_r|\\ |\Delta\theta|=|\mathrm{rem}[(\theta_{\mathrm{f}}-\theta),2\pi]|,|\Delta v_\theta|=|v_{\theta_{\mathrm{f}}}-v_\theta|\\ |\Delta z|=|z_{\mathrm{f}}-z|,\quad |\Delta v_z|=|v_{z_{\mathrm{f}}}-v_z|\end{cases} \tag{26}$$

Eq.(26) indicates the deviation between the current state of the controlled spacecraft and the expected state, the subscript "f" indicates the expect-

ed terminal state, and rem(p, q) returns the remainder after division of p by q.

In addition, after the spacecraft meets the terminal constraints, it may deviate from the expected state due to further collision avoidance control. In this case, to avoid frequent switching of the controller, it needs to design the start and stop control limits for each spacecraft, and the stop limit is less than the start limit. If the any one of the state deviations is greater than the starting limit, the controller is switched on. When all state deviations are less than the stop limit, the controller is cut off.

4 Simulation

This section provides two examples to verify the proposed neural network for the fuel optimal solution, and the proposed intelligent controller for collision avoidance. Assume that the mass is $m=270$ kg, the specific impulse of electric thrusters is $I_{sp}=3\,000$ s, and the maximum thrust magnitude is $T_{max}=100$ m·N. Nominal orbit elements $[a, e, i, \Omega, \omega, \varphi]=[7\,378\text{ km}, 0.1, 0, 0, 0, 0]$. The maximum transfer time is set to be 4.84×10^5 s. Similar to Ref.[21], the parameters of APF and control limits applied in this example are listed in Table 1.

Table 1 Parameters of APF and control limits

APF parameter	Start limit parameter	Stop limit parameter
	$r_{sta}=200$ m	$r_{sto}=100$ m
$k=3.2\times10^4$	$\theta_{sta}=1°$	$\theta_{sto}=1°$
$L=1$ km	$z_{sta}=200$ m	$z_{sto}=100$ m
$d_0=20$ km	$v_{rsta}=1.0$ m/s	$v_{rsto}=0.8$ m/s
$da_0=10$ m	$v_{\theta sta}=0.2(°)$/s	$v_{\theta sto}=0.15(°)$/s
	$v_{zsta}=1.0$ m/s	$v_{zsto}=0.8$ m/s

4.1 Neural network performance

In this subsection, the Monte Carlo tests with 100 satellites are used to verify the proposed neural network controller. The deviations between initial orbit and nominal orbit of each spacecraft are uniformly randomly distributed as $\Delta a_0\in[0, 100\text{ km}]$, $\Delta e_0\in[-0.1, 0]$, $\Delta\omega_0\in[0, 360°]$, and $\Delta\varphi_0\in[0, 360°]$. The expected transfer phases are also uniformly randomly distributed as $\Delta\varphi_f\in[0, 360°]$. When all state deviations are less than the stop constraint, the phasing control is stop. The stop limits of the control are listed in Table 1.

The terminal phase error and the fuel error of the proposed minimum-fuel neural network controller in the 100 tests are shown in Table 2 and Fig.4. Table 2 shows that the average terminal phase error is 0.347 1°. Compared with the indirect method, the increased fuel consumption of the proposed neural network method is less than 1%. However, the mean computational time of the minimum-fuel neural network controller is 0.009 5 s, which is suitable for on-orbit autonomous control.

Table 2 Terminal phase error and fuel error of the proposed neural network controller

Average terminal phase error/(°)	Minimum fuel error/%	Maximum fuel error/%	Average fuel error/%
0.347	0.237	0.938	0.706

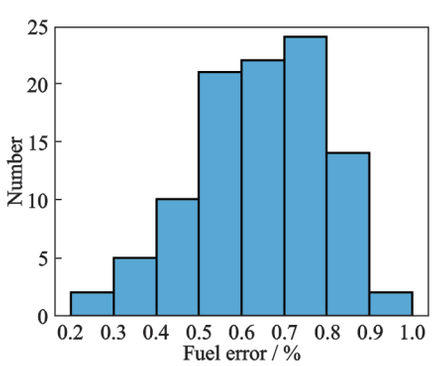

Fig.4 Fuel index error distribution

4.2 Constellation initialization simulation

In this subsection, a constellation initialization control is considered for the multi-spacecraft orbit phasing control method. A series of spacecraft are distributed in series on the same orbit plane, and the goal is to make the spacecraft realize phase uniform distribution in a given order in orbit.

The orbital elements of the spacecraft are the same as that of the nominal initial orbit except the

initial phase. These spacecraft are initially numbered from large to small according to their initial phase φ, ranging from 1 to 60 with the interval phase 0.17°. At the initial time, the phase of the 1st spacecraft is 354.9°, and that of the 60th spacecraft is 5.1°.

Note that the final distribution order of spacecraft is different from its initial order. The spacecraft may collide with each other in the control process. To avoid collision, the boundary of the APF is set to be 20 km. When the distance between two spacecraft is less than 1 km, the collision is considered. The parameters of APF and the control limit of spacecraft are listed in Table 1. The expected final order of spacecraft is $\mathbf{Num}_E$, i.e.

$$\begin{aligned}\mathbf{Num}_E=[&1\ \ 16\ \ 54\ \ 40\ \ 38\ \ 41\ \ 11\ \ 10\ \ 55\ \ 8;\cdots\\ &35\ \ 56\ \ 32\ \ 28\ \ 44\ \ 17\ \ 50\ \ 59\ \ 37\ \ 46;\cdots\\ &51\ \ 31\ \ 34\ \ 22\ \ 24\ \ 47\ \ 29\ \ 45\ \ 39\ \ 25;\cdots\\ &4\ \ 6\ \ 36\ \ 14\ \ 15\ \ 58\ \ 33\ \ 27\ \ 26\ \ 13;\cdots\\ &23\ \ 20\ \ 43\ \ 52\ \ 53\ \ 18\ \ 9\ \ 3\ \ 49\ \ 12;\cdots\\ &57\ \ 30\ \ 21\ \ 19\ \ 12\ \ 7\ \ 5\ \ 42\ \ 48\ \ 60]\end{aligned}$$

where $\mathbf{Num}_E$ is the row vector arranged from left to right.

When the gain coefficient $k=3.2\times10^4$, at different time instants in the control process, the positions of spacecraft are shown in the Fig.5. After 4.84×10^5 s, the constellation initialization is completed. The curve of the minimum distance among all spacecraft in the whole control process is plotted in Fig.6. The minimum distance is 1.520 km, which is greater than the collision limit (i.e., 1 km). The fuel consumption of each spacecraft with collision avoidance is 0.025—0.233 kg, and the total fuel consumption is 6.763 kg.

For different gain coefficients k, the minimum distance and the total fuel consumption are listed in Table 3. When the gain coefficient $k=0$, it is equivalent to ignoring the APF in the whole control process. The minimum distance and the fuel consumption increases with increasing gain coefficient k. For a small k, the minimum distance between spacecraft may be less than the collision limit.

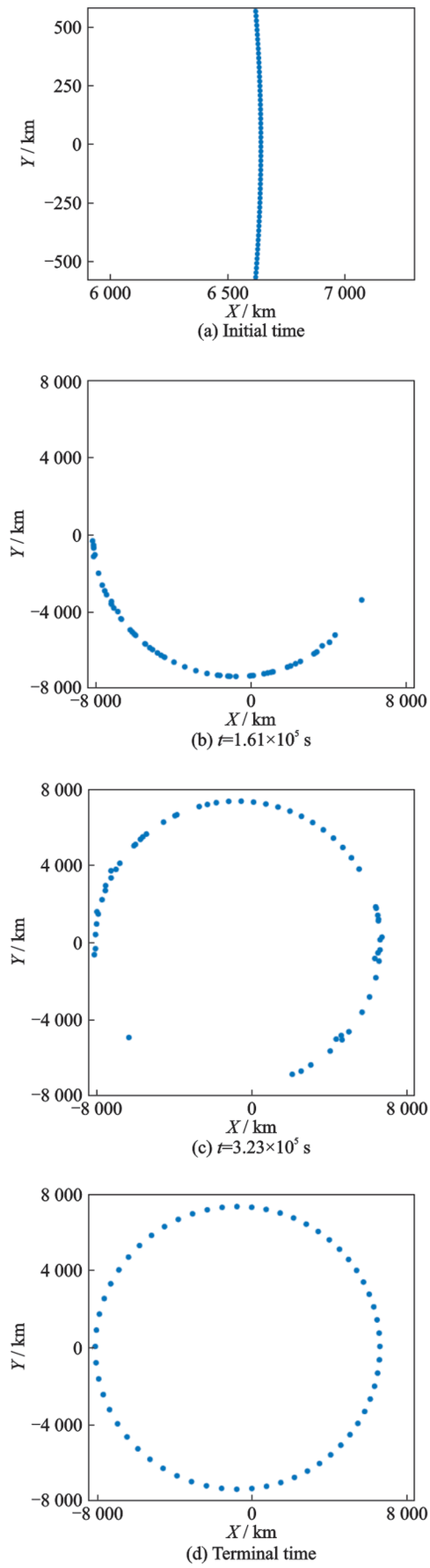

Fig.5 Spacecraft positions at different time instants

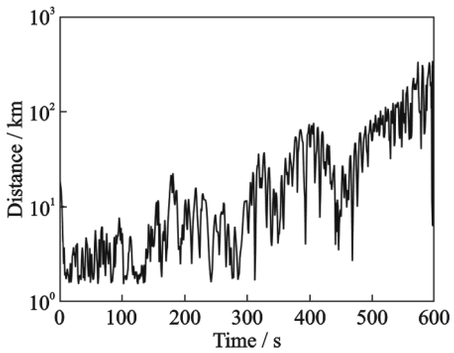

Fig.6 Minimum distance among all spacecraft

Table 3 Minimum distance and total fuel consumption for different k

Gain coefficient k	Minimum distance / m	Totl fuel consumption / kg
0	0.313	6.205
3.2×10^3	0.629	6.515
3.2×10^4	1.520	6.753
3.2×10^5	1.598	6.821

5 Conclusions

A new intelligent multi-spacecraft orbit phasing control method is developed by simultaneously considering fuel optimization and collision avoidance. Firstly, the indirect method associated with the homotopy technique is used to generate the optimal control database. Then, two neural networks are constructed to obtain a minimum-fuel neural network controller that can generate the fuel-optimal control according to the current and expected state. In addition, based on the APF, a collision avoidance method by adjusting the semi-major axis is proposed to handle the collision problem. Finally, the intelligent control is obtained by combining the minimum-fuel neural network and the collision-avoidance method.

The numerical results show that the proposed minimum-fuel neural network is able to predict the optimal thrust magnitude and thrust direction. For the phasing problem, the fuel consumption increases by less than 1% compared with the optimal solution. For the constellation initialization, the increase of fuel consumption of the proposed controller is also reasonable compared with the optimal control without the collision constraint. However, the minimum distance of the proposed method can meet the collision limit.

References

[1] KLUEVER C A. Optimal low-thrust interplanetary trajectories by direct method techniques[J]. Journal of the Astronautical Sciences, 1997, 45(3): 247-262.

[2] CHUANG C H, GOODSON T, HANSON J. Fuel-optimal, low-and medium-thrust orbit transfers in large numbers of burns[C]//Proceedings of Guidance, Navigation, and Control Conference. [S.l.]: [s.n.], 1994: 972-982.

[3] PETROPOULOS A E, LONGUSKI J M. Shape-based algorithm for automated design of low-thrust, gravity-assist trajectories[J]. Journal of Spacecraft and Rockets, 2004, 41(5): 787-796.

[4] GUO T, JIANG F, LI J. Homotopic approach and pseudospectral method applied jointly to low thrust trajectory optimization[J]. Acta Astronautica, 2012, 71: 38-50.

[5] PAN B, LU P, PAN X, et al. Double-homotopy method for solving optimal control problems[J]. Journal of Guidance, Control, and Dynamics, 2016, 39(8): 1706-1720.

[6] JIANG F, TANG G, LI J. Improving low-thrust trajectory optimization by adjoint estimation with shape-based path[J]. Journal of Guidance, Control, and Dynamics, 2017, 40(12): 3280-3287.

[7] CHENG L, WANG Z, JIANG F. Real-time control for fuel-optimal moon landing based on an interactive deep reinforcement learning algorithm[J]. Astrodynamics, 2019, 3(4): 375-386.

[8] YIN S, LI J, CHENG L. Low-thrust spacecraft trajectory optimization via a DNN-based method[J]. Advances in Space Research, 2020, 66(7): 1635-1646.

[9] SÁNCHEZ-SÁNCHEZ C, IZZO D. Real-time optimal control via deep neural networks: Study on landing problems[J]. Journal of Guidance, Control, and Dynamics, 2018, 41(5): 1122-1135.

[10] CHENG L, JIANG F, WANG Z, et al. Multi-constrained real-time entry guidance using deep neural networks[J]. IEEE Transactions on Aerospace and Electronic Systems, 2020, 57(1): 325-340.

[11] IZZO D, ZTÜRK E. Real-time guidance for low-thrust transfers using deep neural networks[J]. Journal of Guidance, Control, and Dynamics, 2021, 44(2): 315-327.

[12] MORGAN D, CHUNG S J, HADAEGH F Y. Model predictive control of swarms of spacecraft using sequential convex programming[J]. Journal of Guidance, Control, and Dynamics, 2014, 37(6): 1725-1740.

[13] WANG Z, XU Y, JIANG C, et al. Self-organizing control for spacecraft clusters using artificial potential function in terms of relative orbital elements[J]. Aerospace Science and Technology, 2018, 84: 799-811.

[14] RENEVEY S, SPENCER D A. Establishment and control of spacecraft formations using artificial potential functions[J]. Acta Astronautica, 2019, 162: 314-326.

[15] ZHANG J, YE D, BIGGS J D, et al. Finite-time relative orbit-attitude tracking control for multi-spacecraft with collision avoidance and changing network topologies[J]. Advances in Space Research, 2019, 63: 1161-1175.

[16] ZHUANG M, TAN L, LI K, et al. Fixed-time position coordinated tracking control for spacecraft formation flying with collision avoidance[J]. Chinese Journal of Aeronautics, 2021, 34(11): 182-199.

[17] HUANG X, YAN Y, ZHOU Y. Underactuated spacecraft formation reconfiguration with collision avoidance[J]. Acta Astronautica, 2016, 131: 166-181.

[18] YU Y, YUE C, LI H, et al. Autonomous low-thrust control of long-distance spacecraft clusters using artificial potential function[J]. Journal of The Astronautical Sciences, 2021, 68: 71-95.

[19] FAN Z, HUO M, QI N, et al. Initial design of low-thrust trajectories based on the Bezier curve-based shaping approach[J]. Proceedings of the Institution of Mechanical Engineers, Part G: Journal of Aerospace Engineering, 2020, 234(11): 1825-1835.

[20] GOLDSTEIN H, POOLE C, SAFKO J. Classical mechanics[M]. 3rd ed. Massachusetts: Addison-Wesley, 2001: 153-154.

[21] LI S, LIU C, SUN Z. Finite-time distributed hierarchical control for satellite cluster with collision avoidance[J]. Aerospace Science and Technology, 2021, 114: 106750.

Acknowledgements This work was supported in part by the National Natural Science Foundation of China (No. 11772104), in part by the Key Research and Development Plan of Heilongjiang Province (No. GZ20210120), and in part by the Fundamental Research Funds for the Central Universities.

Authors Mr. **LI Jian** received the B.S. degree in aerospnaiace science and technology in 2020 from Harbin Institute of Technology, Harbin, China. He is currently pursuing the M.S. degree in aerospace science and technology at the Research Center of Satellite Technology, Harbin Institute of Technology. His research areas are low thrust trajectory optimization and intelligent control.

Prof. **ZHANG Gang** received the B.S. degree from the School of Mathematics at Jilin University, Changchun, China, in 2007, and the Ph.D. degree in aerospace engineering from Harbin Institute of Technology, Harbin, China, in 2012. He is currently a professor at the Research Center of Satellite Technology, Harbin Institute of Technology. His research areas are orbit mechanics, orbit rendezvous, and trajectory optimization.

Author contributions Mr. **LI Jian** designed this research, compiled the model, conducted the simulation, analyzed the results, and wrote the manuscript. Prof. **ZHANG Gang** contributed to the background, methods and writing of the final paper. All authors commented on the draft and approved the submission.

Competing interests The authors declare no competing inrests.

(Production Editor: ZHANG Huangqun)

考虑碰撞避免的多航天器智能轨道相位控制

历 鉴, 张 刚

(哈尔滨工业大学卫星技术研究所, 哈尔滨 150080, 中国)

摘要: 提出了一种同时考虑燃料优化和碰撞避免的多航天器智能小推力轨道相位控制方法。首先, 利用间接法与同伦法生成最小燃料轨道相位转移控制数据库, 并利用数据库训练了代表最小燃料解的深度神经网络。其次, 为了避免多个航天器之间发生碰撞, 利用人工势函数设计了一种碰撞避免控制器。最后, 将最小燃料神经网络控制器与碰撞避免控制器相结合, 提出了一种智能轨道相位控制方法。仿真结果表明, 所提出的智能轨道相位控制方法对于考虑碰撞避免的多星星座初始化控制是有效的。

关键词: 轨道相位控制; 小推力; 深度神经网络; 碰撞规避